H_2O_2. First, values of k_{1y} for (1)$Fe^{III}(X)_2$ and (1)-$Mn^{III}(X)_2$ are comparable only at high pH (II^- decomposition). As the pH decreases, (1)$Fe^{III}(X)_2$ becomes a much better catalyst (Figure 3). These differences in pH dependences of k_{1y} relate to the pH dependences of $E°'$ potentials for (1)$Fe^{III}(X)_2$ (Scheme I) and (1)-$Mn^{III}(X)_2$ (Scheme VI) species. Thus, $E°'$ for $1e^- + (1)Mn^{IV}(OH)_2 \rightarrow (1)Mn^{III}(OH)_2$ and $1e^- + (1)Fe^{IV}(OH)_2 \rightarrow (1)Fe^{III}(OH)_2$ differ by but 30 mV ($\Delta\Delta G°$ = 0.5 kcal/mol), and k_{1y} for reactions of (1)$Mn^{III}(OH)_2$ and (1)$Fe^{III}(OH)_2$ with hydroperoxides are comparable (Figure 3). The $E°'$ for $1e^-$ reduction of (1)Mn^{IV}(O-H)(H_2O) exceeds that for (1)$Fe^{IV}(OH)(H_2O)$ by 70 mV ($\Delta\Delta G°$ = 1.6 kcal/mol), whereas $E°'$ for $1e^-$ reduction of (1)$Mn^{IV}(H_2O)_2$ is more positive than that for (1)-$Fe^{IV}(H_2O)_2$ by 130 mV ($\Delta\Delta G°$ = 3.0 kcal/mol) and the reaction of (1)$Mn^{III}(H_2O)_2$ with hydroperoxide cannot be determined over spontaneous decomposition of hydroperoxide. General catalysis with (Porph)$Fe^{III}(X)_2$ catalysts is seen only with the IIH_2^+ species (Scheme II), and reactions through the IIH_2^+ species cannot be detected with (Porph)$Mn^{III}(X)_2$ catalysts. It is, therefore, not surprising to find that the reactions of hydroperoxides with (1)$Mn^{III}(X)_2$ and (2)$Mn^{III}(X)_2$ are not subject to general-acid/base catalysis by H_2O, (oxygen base)/(oxygen acid) pairs, not (nitrogen base)/(nitrogen acid) pairs at any pH.

The ratios of the rate constants, at a given pH, for the reactions of $(Ph)_2(CH_3OCO)COOH$, *t*-BuOOH, and $Ph(CH_3)_2COOH$ with (1)$Mn^{III}(X)_2$ and (1)$Fe^{III}(X)_2$ are comparable, suggesting hydroperoxide O–O bond homolysis. This is supported by the products obtained from reaction of *t*-BuOOH with (1)$Mn^{III}(X)_2$.

With imidazole, (1)$Mn^{III}(X)_2$ forms a monoligated species which reacts with alkyl hydroperoxides (eq 29) with a rate constant, k_{Im}, exceeding k_{1y} for the reaction with (1)$Mn^{III}(X)_2$ by 10–100-fold.

$$-d[YOOH]/dt = k_{Im}[(1)Mn^{III}(X)(\text{"imidazole"})][YOOH] \quad (29)$$

This work was supported by grants from the National Institutes of Health and the National Science Foundation.

Second-Moment Scaling and Covalent Crystal Structures

STEPHEN LEE

University of Michigan, Department of Chemistry, 930 North University Avenue, Ann Arbor, Michigan 48109-1055

Received April 18, 1991 (Revised Manuscript Received July 22, 1991)

In recent years the molecular orbital theory, originally developed to study small organic and inorganic molecules, has been successfully applied to the study of the infinite arrays of atoms found in extended solids.[1] In much of this work, arguments based on simple quantum mechanical models have been used to account for the structures and properties of these large and at times dauntingly complex chemical systems. Clear examples of this approach can be found in the work of J. K. Burdett, R. Hoffmann, and M. H. Whangbo. Their contributions have been reviewed recently.[1] The research reported in this Account is heavily influenced by the viewpoints of the aforementioned researchers.

In this Account we show how a modified Hückel theory allows one to make accurate predictions about the structures of covalently bonded extended solids. This modification was suggested independently in earlier work by D. G. Pettifor and R. Podloucky and in work by J. K. Burdett and me.[2] The modification itself has recently been investigated with renewed vigor by D. Pettifor's group and our own group at Michigan.[2] We call our method second-moment scaling. In order to understand the basis of second-moment scaling, we consider first the Hückel theory as it was originally applied to unsaturated hydrocarbons.

Hückel Theory

In Hückel theory one assumes that the principal force governing covalent bonds is the overlap of the respective atomic orbitals. Formally, this corresponds to solving the equation $H\psi = E\psi$, where the off-diagonal elements of the Hückel Hamiltonian, H_{ij}, follow the Wolfsberg–Helmholtz approximation,[3] $H_{ij} = KS_{ij}(H_{ii} + H_{jj})$, S_{ij} is the overlap integral, K is a proportionality constant, and the H_{ii} values are taken from compendiums of atomic parameters.[4] In this Account we will generally assume that the S_{ij} values depend on the orientations and distances of the respective atomic orbitals.

One of the best known applications of Hückel theory is for unsaturated hydrocarbon ring systems such as the cyclopropenium cation (1), benzene (2), and the hypothetical cyclobutadiene dianion 3. It is well-known that the triangular form, 1, is stable only as a cation and the hexagonal form, 2, is stable as a neutral molecule, while

Stephen Lee did his undergraduate work at Yale University and his graduate work at the University of Chicago with J. K. Burdett. He did his postdoctoral work with G. Hillhouse, J. Rouxel, and W. Jeitschko. Since 1988, he has been at the University of Michigan, where he is currently an Assistant Professor of Chemistry.

(1) (a) Hoffmann, R. *Solids and Surfaces: A Chemist's View of Bonding in Extended Structures*; VCH Publishers: New York, 1988. (b) Burdett, J. K. *Prog. Solid State Chem.* **1984**, *15*, 173. (c) Whangbo, M.-H. In *Crystal Chemistry and Properties of Materials with Quasi-One Dimensional Structure*; Rouxel, J., Ed.; Reidel: Dordrecht, 1986; p 27.

(2) Early applications of the second-moment-scaling hypothesis (a) for AB (main group and transition metal) phases: Pettifor, D. G.; Podloucky, R. *Phys. Rev. Lett.* **1984**, *53*, 1080. (b) For the Peierls distortion: Burdett, J. K.; Lee, S. *J. Am. Chem. Soc.* **1985**, *107*, 3063. More recent work: (c) Cressoni, J. C.; Pettifor, D. G. *J. Phys.: Condens. Matter*, submitted for publication. (d) Lee, S. *J. Am. Chem. Soc.* **1991**, *113*, 101. (e) For elemental structures: Lee, S. *J. Am. Chem. Soc.*, submitted for publication.

(3) Wolfsberg, M.; Helmholtz, L. *J. Chem. Phys.* **1952**, *20*, 837.

(4) Many important atomic parameters are reported in the following: (a) Hoffmann, R. *J. Chem. Phys.* **1963**, *39*, 1397. (b) Hoffmann, R.; Anderson, A. B. *J. Chem. Phys.* **1974**, *60*, 4271. (c) Hoffmann, R.; Rossi, A. R. *Inorg. Chem.* **1975**, *14*, 365. (d) Hay, P. J.; Thibeault, J. C.; Hoffmann, R. *J. Am. Chem. Soc.* **1975**, *97*, 4884. (e) Hoffmann, R.; Elian, M. *Inorg. Chem.* **1975**, *14*, 1058. (f) Hoffmann, R.; Summerville, R. H. *J. Am. Chem. Soc.* **1976**, *98*, 7240. (g) Komiya, S.; Albright, T. A.; Hoffmann, R.; Kochi, J. K. *J. Am. Chem. Soc.* **1977**, *99*, 8440. (h) Thorn, D. L.; Hoffmann, R. *Inorg. Chem.* **1978**, *17*, 126. (i) Hughbanks, T.; Hoffmann, R.; Whangbo, M.-H.; Stewart, K. R.; Eisenstein, O.; Canadell, E. *J. Am. Chem. Soc.* **1982**, *104*, 3876. (j) Chen, M. M. L.; Hoffmann, R. *J. Am. Chem. Soc.* **1976**, *98*, 1647.

0001-4842/91/0124-0249$02.50/0

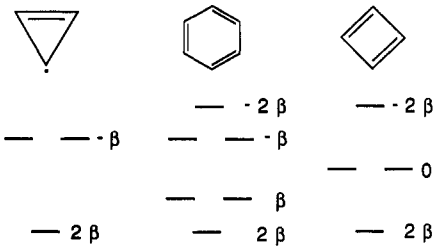

Figure 1. The π molecular orbital energies for the cyclopropenium cation, benzene, and square cyclobutadiene.

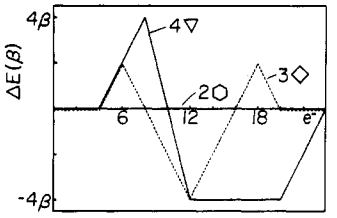

Figure 2. Differences in energy for the π systems of 1–3 as functions of the number of π electrons. See text for figure conventions.

the square form, 3 (by the Hückel $4N + 2$ rule), would be more stable as the dianion than the neutral species.

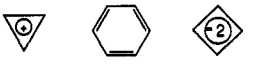

1 2 3

The Hückel molecular orbital diagrams for these three systems can be used to account for the above set of facts. These molecular orbital diagrams are shown in Figure 1. It may be seen that in each case the stable chemical systems contain the exact number of electrons required to fill all bonding and nonbonding orbitals. It is of interest, however, to reanalyze these molecular orbitals in terms of total electronic energy. To do so we need to compare equivalent numbers of atoms. In this example it is convenient to compare the π orbitals of exactly 12 carbon atoms. This is because molecules 1–3 contain respectively three, six, and four carbon atoms and each of these three numbers is a factor of 12. Therefore we will compare the electronic energies of four triangles, 1, two hexagons, 2, and three squares, 3. For example, with eight π electrons the four triangles have a Hückel electronic energy of 16β ($8 \times 2\beta$, see Figure 1), the two hexagons have an energy of 12β ($4 \times 2\beta + 4 \times 1\beta$), and the three squares have a total energy of 12β ($6 \times 2\beta + 2 \times 0\beta$).

In the same manner we may consider different numbers of π electrons. It is convenient to plot these data in the graphical manner shown in Figure 2. In Figure 2 the curve labeled as four triangles corresponds to the difference in binding energy between the four triangles and the two hexagons as a function of the total number of π electrons in the system. We adopt the convention that when the curve is positive, the triangular form is more stable. Similarly, the curve labeled three squares represents the difference in energy between the square and hexagonal forms. We may use the curves in Figure 2 to deduce the Hückel prediction as to which molecular form is the most stable one at any given π-electron count. The most stable form corresponds to the curve that is the most positive at the electron count in question. Thus at eight electrons/12 carbon atoms the triangular form is most stable; at 12 electrons the hexagonal form is most stable; and at 18 electrons the square form is most stable. When one divides these numbers by the numbers of triangles, hexagons, or squares, one sees that these three electron counts correspond to the π-electron count of the experimentally known cyclopropenium cation, benzene, and S_2N_2 (which is isoelectronic with $C_4H_4^{2-}$).

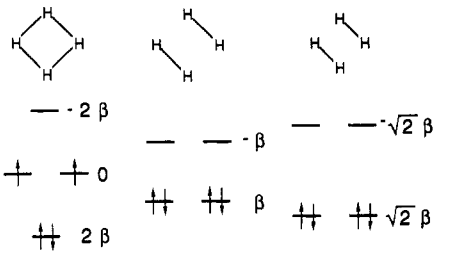

Figure 3. The molecular orbital energies for the square H_4 molecule and for two H_2 molecules. The left and middle columns have a constant resonance integral between bonded H atoms. The left and right columns have a constant variance for their molecular orbital energies.

Coordination Problem and Second-Moment Scaling

Predictions based on the total Hückel electronic energy are reasonably reliable when the bond breakage or formation is not an integral part of the structural question under study.[5] For example, in the systems discussed in the previous section, the number of bonds was invariant among the three 12 carbon atom systems.

Hückel energies are not reliable, however, when the total number of bonds is not conserved.[5] For example, consider the four hydrogen atoms aligned in a square as opposed to two pairs of hydrogen dimers. The Hückel energies of these two arrangements are shown in Figure 3. It may be seen that Hückel theory predicts that the tetramer of hydrogen atoms is of the same energy as the pair of dimers. This of course is completely wrong. The source of this error can be understood if one recalls that Hückel energies are proportional to the overlap integrals, S_{ij}, and that the Hückel Hamiltonian contains no repulsive interactions. The H_4 tetramer is therefore automatically conferred an additional stabiilty over the pair of H_2 dimers since the hydrogen atoms are closer to one another in the former geometry. This greater proximity leads to larger overlap integrals, to lower energy bonding orbitals, and to higher energy antibonding orbitals. Therefore, there is an overall increase in the variance (where variance $= \sum_i (E_i - E_{avg})^2$) for the molecular orbital energies E_i.

It is difficult to suggest a good method of electronic structure calculations that will both remove the problem of different coordination numbers and at the same time leave the theory comparatively simple. However, we and others have made an ad hoc suggestion to circumvent this coordination problem.[2] We suggest that one should scale the molecular orbital diagrams so that variance is a constant. For example, in comparing the H_4 tetramer to the pair of dimers, we adjust the β interaction in the pair of dimers to the values shown at the right in Figure 3. With these new values the variance for the H_4 tetramer equals the variance for the pair of dimers. It may be seen that, with this scaling, the pair of dimers is of lower energy than the tetramer,

(5) For a discussion of this coordination number problem, see: Burdett, J. K. *Structure Bonding* **1987**, *65*, 29.

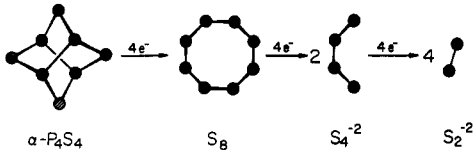

Figure 4. The effect of oxidation and reduction on the structure of eight S atoms. Note that P_4S_4 is isoelectronic with S_8^{4+}.

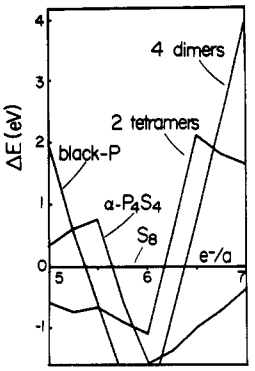

Figure 5. Differences in energy between black phosphorus, α-P_4S_4, S_8, $2S_4^{2-}$, and $4S_2^{2-}$ molecules as functions of the average number of valence electrons per atom (e^-/atom). See discussion, in text, of Figure 2 for figure conventions. The calculation used the atomic parameters for S reported in ref 4j. All calculations were (second-moment) scaled to that calculated for experimentally observed S_8 molecules.[6a]

as is experimentally known to be true.

We call the above procedure second-moment scaling. We could as well have called it variance scaling. This is because we always compare the same types of atoms in any given calculation. Therefore, the mean of the molecular orbital energies is constant, and thus, fixing the second moment, μ_2 ($\mu_2 = \sum_{i=1}^{n}(E_i^2/n)$, where the E_i are the molecular orbital energies and n is the total number of molecular orbitals), is equivalent to fixing the variance.

Elemental Structures

As a simple example of the method, consider the change in structure induced in eight sulfur atoms as we reduce or oxidize the system. These structures are illustrated in Figure 4.[6] We include α-P_4S_4 as we shall assume throughout this Account that isoelectronic compounds involving elements from the same row in the periodic table are isostructural. In this case, for example, we assume α-P_4S_4 to be isostructural with S_8^{4+}. It may be seen that each of these structures contains a different number of bonds. Therefore, we need to scale the second moments so that they are all equal. In practice we do this scaling by actually shrinking or expanding the various molecules in a uniform way so as to equate the μ_2's. We leave bond angles unchanged by the geometrical transformation. We also consider the overlap integrals between all atoms and all orbitals. In Figure 5 we show the results of our Hückel calculations on these systems. One may note that the results in Figure 5 correspond to the experimental findings shown in Figure 4. Furthermore, in Figure 5 we have included the black phosphorus structure, which is the most stable form of phosphorus.[6a] Black phosphorus is an extended solid wherein every phosphorus atom has three bonds. Therefore, we are comparing in Figure 5 the energies of an extended solid to those of molecules. The latter systems are treated by molecular orbital methods, whereas the former are determined through band calculations. However, this difference is only technical. Both types of calculations depend identically on the same chemical assumptions.

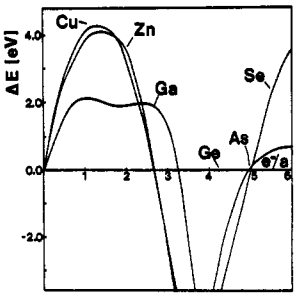

Figure 6. Differences in energy between the Cu (fcc), Zn (hcp), Ga, Ge (diamond), As, and Se structures as functions of e^-/atom. The calculational results are all based on full band calculations with the Ge parameters reported in ref 4h. All calculations were scaled to the experimentally observed Ge structure. See discussion, in text, of Figure 2 for figure conventions.

Li 3	Be 3									B 3	C 3	N 3	O 3	F 3
											Si 3	P 3	S 3	Cl 3
V 1	Cr 1	Mn 2	ferromagnetic				Cu 2,3	Zn 2,3	Ga 3	Ge 3	As 3	Se 3	Br 3
Nb 1	Mo 1	Tc 2	Ru 2	Rh 2	Pd 2	Ag 2,3	Cd 2,3	In 4	Sn 3,4	Sb 3,4	Te 3,4	I 3
Ta 1	W 1	Re 2	Os 2	Ir 2	Pt 2	Au 2,3		Tl 4	Pb 4	Bi 4	Po 4	

1 = s & d model; 2 = s,p, & d model; 3 = s & p model;
4 = s & contracted p model

Figure 7. Elements whose elemental crystal structures have been rationalized through second-moment-scaled Hückel theory. Calculations rely on the indicated valence orbitals. For specific atomic parameters, see refs 4. In the case of In, the observed fcc distortion[6a] changes the energy by only 0.02 eV/atom. We therefore cannot rationalize this subtle distortion.

Calculations carried out independently in our group and by D. G. Pettifor and J. C. Cressoni have shown that this technique can be broadly applied to the elemental structures of much of the periodic table.[2] For example, we can consider the crystal structures of elements 29–34 (Cu, Zn, Ga, Ge, As, and Se).[6a] The first three elements in this series are metals. Cu has the face centered cubic structure, Zn has the hexagonal closest packed structure, and Ga has an unusual 7-coordinate structure. Germanium adopts the diamond structure, whereas As and Se have, respectively, three and two nearest neighbors per atom. These last two elements, therefore, both obey the octet rule. In Figure 6 we show our calculations comparing these structures. It may be seen that, at each integral electron count, the prediction based on Hückel theory corresponds to the experimentally determined structure type.

In a similar way we can consider the structures of other elements. Indeed our method correctly accounts for the structures of the elements shown in Figure 7.[2e] Several of the actual results for the main-group elements are shown in Figure 8. (We discuss the transition metals in a later section.)

It should be noted that, for our calculational technique to be effective, the individual variation in atomic

(6) (a) For elemental structures themselves, see: Donohue, J. *The Structures of the Elements*; Wiley: New York, 1974. (b) For α-P_4S_4: Griffin, A. M.; Minshall, P. C.; Sheldrick, G. M. *J. Chem. Soc., Chem. Commun.* **1976**, *809*. (c) For S_4^{2-} (NaS_2): Tegman, R. *Acta Crystallogr.* **1973**, *B29*, 1463.

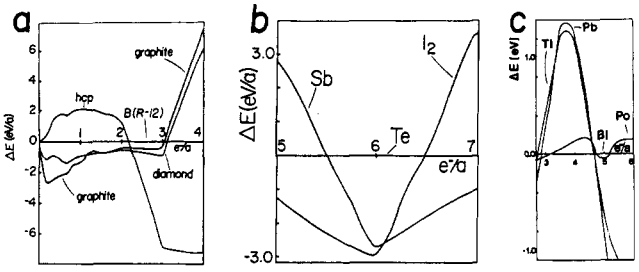

Figure 8. Differences in energy for (a) the Li and Be (both hcp), boron (R-12),[6a] and carbon structures; (b) the structures of Sb, Te, and I; and (c) the Tl (hcp), Pb (fcc), Bi, and Po (simple cubic) structures as functions of e^-/atom. In part a, B parameters were used; in part b, Te parameters were used; and in part c, normal p and contracted s orbitals were used.[2a] See discussion, in text, of Figure 2 for figure conventions. I thank D. Chou and S. Carter for their help in carrying out the calculations.

Hückel parameters must be small between neighboring elements in a given row of the periodic table. It is this small variation that allows us to compare the stability of different structure types as a function of the number of valence electrons, without explicitly accounting for the different types of atoms.

We find, in general, that the parameters developed over the years for extended Hückel theory can be used without change in our calculations.[4] This is important as we therefore do not adjust our atomic parameters to improve the results of our calculations. There is, however, one situation wherein the atomic extended Hückel parameters need to be modified. Such modifications arise if there are atomic orbitals that are halfway between being core and valence orbitals. Examples of such orbitals are the d orbitals of Zn, Cd, and Hg. Another important set of highly contracted orbitals is the s orbitals in Tl, Pb, Bi, and Po. This latter set of orbitals is responsible for the inert-pair effect in these atoms and plays only a small role in structural chemistry.[7] Indeed, some years ago we showed that the structures of the heaviest main-group elements can be rationalized if one ignores these s orbitals entirely.[2b]

One goal of our research program is to use the minimum number of variable parameters possible. Every atomic orbital has two parameters in an extended Hückel or Hückel calculation. These are the Coulombic integral values, H_{ij}, which determine the energy of the atomic orbitals before the onset of molecular interaction, and the Slater exponent, ζ, which controls the size of the atomic orbitals. In the case of the contracted s orbitals and d orbitals discussed above, we have used the following procedure to reduce these two parameters to a single parameter. We select an H_{ii} value that ensures that the partially corelike orbitals lie in a band just below the lower energy edge of the true valence orbitals. As Hückel theory (unlike extended Hückel theory) places the most bonding orbitals at unrealistically low energies, we therefore need to place the core electrons at equally unrealistic values. As a further consequence of this error we must overly contract the partially corelike orbitals to compensate for the energy weighting of the Wolfsberg–Helmholtz approximation. The virtue of this procedure is that in performing our calculations we need to optimize only the Slater exponent, ζ, the Coulombic integral H_{ii} being fixed by the already predetermined true valence orbital atomic parameters. Therefore, in all the calculations reported in this Account there is at most one optimized parameter per set of structures. We believe, therefore, that the results displayed in Figures 6 and 8 are numerically significant.

(7) (a) Pitzer, K. S. *Acc. Chem. Res.* **1979**, *12*, 271. (b) Pykkö, P.; Desclaux, J.-P. *Acc. Chem. Res.* **1979**, *12*, 276. (c) Lohr, L. L., Jr.; Pykkö, P. *Chem. Phys. Lett.* **1979**, *62*, 333.

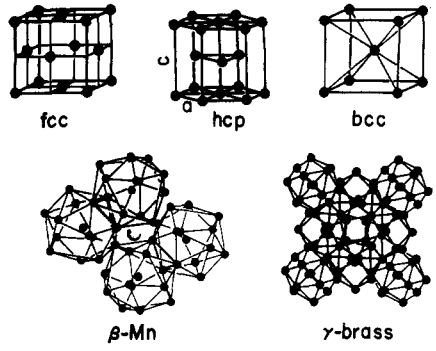

Figure 9. The fcc, hcp, bcc, β-Mn, and γ-brass crystal structures. The ζ, ϵ, and η designations for hcp refer to the ratio of the line segments labeled a and c. See discussion in the text.

Alloys and Metals

We turn now to binary and ternary alloys, i.e., compounds that are mixtures of two and three metallic elements. Over 60 years ago Hume-Rothery observed that one of the crucial variables in rationalizing the structures of these alloys is the average number of valence electrons per atom.[8] Thus in noble-metal and main-group-metal alloys, Hume-Rothery found seven main alloy structure types. The types range from the comparatively simple face-centered cubic (fcc), body-centered cubic (bcc), and hexagonal closest packed (hcp) to the rather complex β-Mn and γ-brass structure types. These structures are illustrated in Figure 9.[9] The hcp structure type is subject to wide variation, and metallurgists often divide this structure into three different branches. In ζ-hcp one finds a true closest packing where every atom has 12 nearest neighbors. This occurs when the hexagonal crystallographic axes a and c are in the ratio $c/a = 1.633$. In addition, metallurgists consider the range of c/a from 1.55 to 1.58 to be ϵ-hcp and the range from 1.77 to 1.88 to correspond to η-hcp. It should be noted that these different hcp structure types can be genuinely different. For example, a sample of Ag_9Cd_1 spontaneously decomposes into two products, one being an ϵ-hcp and the other an η-hcp.

As we stated above, the most important variable for the crystal structure of these alloys is the average number of valence electrons per atom. For example, we can consider the three alloys $Ni_{0.19}Cd_{0.81}$, $Ag_{0.40}Cd_{0.60}$, and $Ag_{0.67}In_{0.33}$, which all crystallize in the γ-brass structure type. As may be seen, there is no fixed relation between stoichiometry and structure type. However, if one calculates the average number of s, p, and d electrons per atom for these three structures, one finds values of, respectively, 11.62, 11.60, and 11.66

(8) (a) Hume-Rothery, W.; Raynor, G. V. *The Structure of Metals and Alloys*; Inst. of Metals: London, 1962. (b) Hume-Rothery, W. In *Phase Stability in Metals and Alloys*; Rudman, P. S., Stringer, J., Jaffee, R. I., Eds.; McGraw-Hill: New York, 1967; p 3.

(9) A discussion of such phases can be found in the following: Pearson, W. B. *The Crystal Chemistry and Physics of Metals and Alloys*; Wiley: New York, 1972.

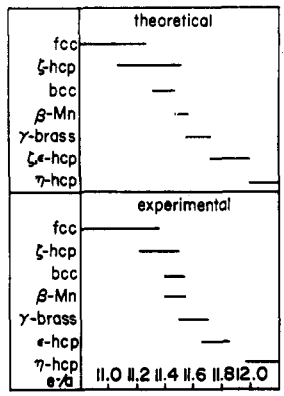

Figure 10. Experimental and theoretically calculated electron ranges for the seven noble-metal Hume-Rothery electron phases. We assume that all structures whose calculated energy comes within 0.025 eV/atom of the lowest energy structure are viable chemical alternatives.

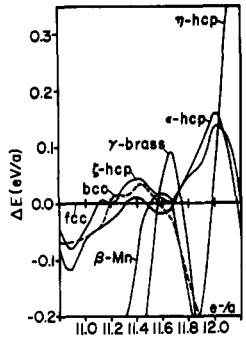

Figure 11. Differences in energy for the seven Hume-Rothery electron phases as functions of s, p, and d e^-/atom. Calculations were scaled to the second moment of Cu_9Si (β-Mn structure type). A highly contracted d orbital with $H_{ii}(3d) = -60.0$ eV and $\zeta(3d) = 2.9$ was used. Other atomic parameters were the same as those used in Figure 6. See text for discussion of these contracted d orbitals.

electrons per atom (e^-/atom). Indeed, all crystals that form in the γ-brass structure type have a number of electrons per atom near this specific value of 11.65. All the other phases discussed above also have a corresponding zone of permissible electron counts. These experimentally determined zones of stability[10] are plotted in Figure 10. Metallurgists call these zones the Hume-Rothery electron concentration rules.

In Figure 11 we show our calculations on these seven structure types.[11] The results in Figure 11 bear a striking similarity to the experimental ranges shown in Figure 10. In both, fcc is the structure favored at low e^-/atom values. At slightly higher e^-/atom values, there is a region where bcc, ζ-hcp, and β-Mn are stable. At 11.65 s, p, and d electrons, γ-brass is most stable. At higher electron counts, first ϵ-hcp is preferred and finally η-hcp is the preferred structure. We display these results fully in Figure 10. It may be seen in this figure that agreement between theory and experiment is excellent.

In order to assess the success of our theoretical model, we need to consider the atomic parameters used in our calculation and their provenance. Our goal has been to minimize the number of variable atomic parameters. Therefore, we have used the same atomic parameters in this curve as those that were used in producing the results in Figure 6. We have, however, by the procedure previously discussed, used one variable parameter. This parameter controls the relative size of the d orbital. The curves shown in Figure 11 use a parameter value that optimizes the agreement between theory and experiment. Given the complexity of Figure 11, it is clear that our data are statistically significant.

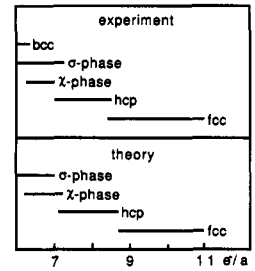

Figure 12. Experimental and theoretically calculated electron ranges for transition-metal binary alloys. We assume that all structures whose calculated energy comes within 0.05 eV/atom of the lowest energy structure are viable chemical alternatives.

In a similar manner, we can consider transition-metal alloys. There are two new major structure types in transition-metal alloys. These are the σ phase and the χ phase. Both structures are described in ref 9. Of especial interest is the χ phase, which not only is the structure of Nb-Os and Hf-Re and other binary alloys but also is the stable form of elemental Mn (α-Mn). This α-Mn structure has the distinction of being the most complicated known elemental structure. It contains 58 atoms in its cubic unit cell. Both this α-Mn structure type (χ phase) and the σ phase are found for electron counts that range between six and seven s, p, and d electrons per atom. At lower electron counts than six, the bcc structure is preferred, whereas at higher electron counts, the hcp and fcc structures predominate. In Figure 12 we compare the results of our calculation to the known electron count ranges for these five structural types. These calculations are based on accepted extended Hückel parameters for Fe. We therefore have adjusted no atomic parameters to improve the fit between theory and experiment. We see in Figure 12 that the agreement between theory and experiment is good. Only at low electron counts does our model fail. For example, the bcc lattice is not the most favored structure at 6 e^-/atom in our calculations. This is in contradiction with the experimental results. We find, however, that if we reduce the effect of the p orbitals, the bcc structure becomes the most favored structure at 5 and 6 e^-/atom.[11] This is a reasonable result. As one approaches the left side of the transition-metal block of the periodic table, the p orbitals rise in energy and play a diminished role in determining the structure of the elements.

Intermetallic Compounds

We may apply this same method to other classes of materials. In this section we consider the family of compounds that have the chemical formula ZA_xB_{2-x}, where Z is an electropositive element such as an alkali metal, an alkaline-earth metal, a lanthanide, a group 4 transition metal, or thorium, whereas A and B are

(10) (a) Hansen, M. *Constitution of Binary Alloys*; McGraw-Hill: New York, 1958. (b) Elliott, R. P. *Constitution of Binary Alloys—First Supplement*; McGraw-Hill: New York, 1965. (c) Shunk, F. A. *Constitution of Binary Alloys: Second Supplement*; McGraw-Hill: New York, 1969. (d) Moffat, W. G. *The Handbook of Binary Phase Diagrams*; Genium, A.; Schenectady, NY, 1987.

(11) Hoistad, L.; Lee, S. *J. Am. Chem. Soc.*, in press.

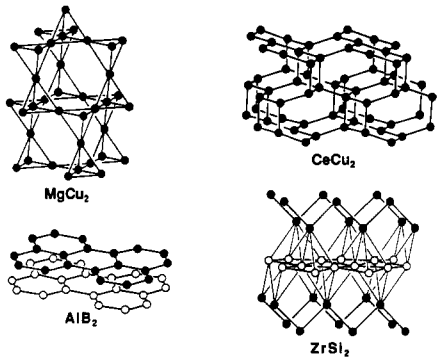

Figure 13. The $MgCu_2$, $CeCu_2$, AlB_2, and $ZrSi_2$ structure types. No electropositive atoms (alkali metal, alkaline earth, etc.) are shown in this figure. Thus, all bonds shown are between main-group atoms. The thin lines in the $ZrSi_2$ structure type indicate the spatial relation of the Si zigzag chains to the Si square lattice.

main-group elements from columns 11–17 of the periodic table.[2d] There are over 1000 comopunds that fulfill the above conditions. Most of these compounds are found in just a handful of structure types. These structure types include the $MgCu_2$, $MoSi_2$, $CeCd_2$, $CeCu_2$, $CaIn_2$, MgAgAs, AlB_2, $ThSi_2$, $ZrSi_2$, $SmSb_2$, and Cu_2Sb structure types.[12] A few of these structures are illustrated in Figure 13.

Using second-moment scaling, it is possible to rationalize the relation between the overall number of valence electrons in a given compound and the structure adopted by that compound. To do so, we consider the electropositive atoms as mere electron donors. Therefore, we do not include the electropositive nuclei in our band calculations. Furthermore, it is assumed in our band calculations that there is only one type of electronegative atom. Therefore, we do not study the effect of different A and B stoichiometries in the ZA_xB_{2-x} compounds. We count our electrons in the following manner. We assume that an electropositive element donates the number of electrons that would correspond to that element's most common oxidation state. Eu, Sr, Ti, Ce, and Th therefore donate 2, 2, 4, 4, and 4 electrons. For main-group atoms, we count only s and p electrons. Thus, for example, MgAgAs has $8e^-/ZA_xB_{2-x}$ unit as $8e^- = 2e^-$ (from Mg) + $1e^-$ (from Ag) + $5e^-$ (from As). In Figure 14 we compare the experimentally determined electron counts for these structure types to the electron counts predicted by our second-moment-scaled band calculations. We see that there are several mismatches between theory and experiment. For example, the experimental electron count range for the $CeCu_2$ structure type is much broader than our theory would have predicted. However, overall agreement is still quite striking.

In the same manner, we can apply second-moment-scaled Hamiltonians to rationalize other families of intermetallic stoichiometries.[13] At the present time we have limited ourselves to covalent chemical systems where electron count plays a predominant role in determining crystal structure types. The results of this and the preceding sections show that within these limitations, whether the system is a molecule, alloy, intermetallic compound, or insulator, second-moment-scaled Hückel theory provides an excellent basis for the rationalization of known crystal structures.

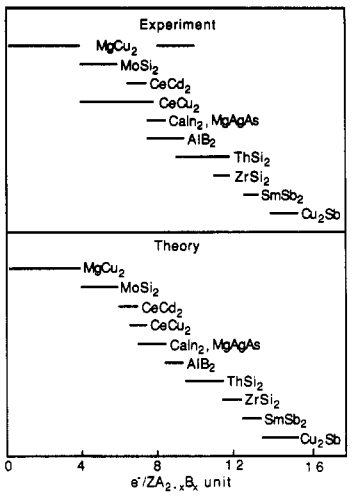

Figure 14. Theoretically calculated and experimental electron ranges for $ZA_{2-x}B_x$ phases. See ref 2d for calculational parameters.

Conclusion

Molecular orbital theory provides a unified picture of the bonding in organic, inorganic, molecular, cluster, crystal, and surface chemistry. Many of the most profound applications of molecular orbital theory such as the Hückel $4N + 2$ rule or the Woodward–Hoffmann rules have relied on molecular orbital theories of the very simplest sort.[14] However, it is often believed that to achieve better computational accuracy one must abandon the simplicity of these original models. We hope that in this Account we have shown that, by appropriately modifying a theory even as basic as Hückel theory, we can achieve a remarkable resonance between theory and experiment. At the moment, our rather straightforward technique of second-moment scaling produces quantitative results as accurate as or more accurate than other, more complex electron structure techniques for purely covalently bonded systems. Our study on the Hume-Rothery rules for noble metals is, to our knowledge, the first complete theoretical study of these well-established rules. We hope that in the future new modifications in Hückel theory will enable the chemist to study an even greater range of structural problems.

I thank members of my research group L. Hoistad, C. Wells, A. Hatta, and E. Fischer for their help and support. This research was partially supported by the donors of the Petroleum Research Fund, administered by the American Chemical Society, and the Rackham Graduate School. This research would not have been possible without computer programs developed by R. Hoffmann, M.-H. Whangbo, T. Hughbanks, S. Wijeyesekera, M. Kertesz, C. N. Wilker, C. Zheng, J. K. Burdett, and G. Miller.

(12) (a) $MgZn_2$: Friauf, J. *Phys. Rev.* **1927**, *29*, 34. (b) $MgCu_2$: Grime, G.; Morris-Jones, W. *Philos. Mag.* **1929**, *7*, 1113. (c) Cu_2Sb: Elander, M.; Hägg, G.; Westgren, A. *Ark. Kemi, Mineral. Geol.* **1935**, *12B*, 1. (d) $MoSi_2$: *Strukturbericht 1*, 740. (e) Fe_2P: Rundqvist, A.; Jellinek, F. *Acta Chem. Scand.* **1959**, *13*, 425. (f) Co_2Si: Geller, S. *Acta Crystallogr.* **1955**, *8*, 83. (g) $CeCu_2$: Larson, A. C. *Acta Crystallogr.* **1961**, *14*, 73. (h) $CeCd_2$: Iandelli, A.; Ferro, R. *Gazz. Chim. Ital.* **1954**, *84*, 463. (i) MgAgAs: Nowotny, H.; Sibert, W. *Z. Metallkd.* **1941**, *33*, 391. (j) $ThSi_2$: Brauer, G.; Mitius, A. *Z. Anorg. Allg. Chem.* **1942**, *345*, 249. (k) $ZrSi_2$: Vaughn, P. *Am. Crystallogr. Assoc. Summer Meeting* **1955**, 8. (l) Villars, P.; Calvert, L. D. *Pearson's Handbook of Crystallographic Data for Intermetallic Phases*; Am. Soc. Metals: Metals Park, OH, 1985.

(13) Hoistad, L.; Lee, S., unpublished results.

(14) Woodward, R. B.; Hoffmann, R. *The Conservation of Orbital Symmetry*; Verlag Chemie: Weinheim, FRG, 1970.